AD-A190 239 HIGH TEMPERATURE SUPERCONDUCTIVITY(U) NAVAL RESEARCH LAB WASHINGTON DC M OSOFSKY 14 DEC 87 1/1

UNCLASSIFIED F/G 20/3 NL

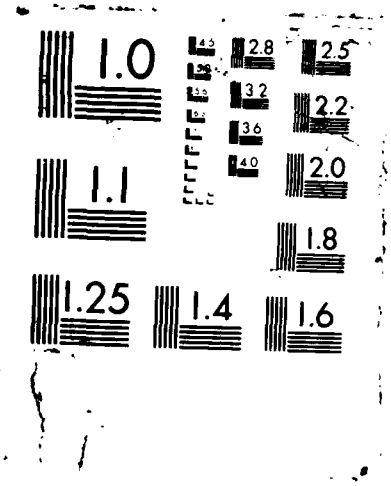
1.0
1.1
1.25
1.4
1.6
1.8
2.0
2.2
2.5
2.8
3.2
3.6
4.0

(2)





# High Temperature Superconductivity

Final Report

ONT Post-doctoral Fellowship

at the Naval Research Laboratory

Michael Osofsky



John Claassen (advisor) _____



December 14, 1987

Soon after the discovery of superconductivity at 30K and 95K in the $La_{2-x}Ba_xCuO_4$ and $YBa_2Cu_3O_7$ systems[1,2] last year my research efforts were diverted to the new field of high temperature superconductivity. This report will be presented in three parts. The first part describes our early studies of the La-M-Cu-O (M=La,Ba,Sr and Pb) system. The second part discusses the $YBa_2Cu_3O_7$ system and the third part deals with the question of superconductivity at temperatures around 200K in the $YBa_2Cu_3O_7$ system.

## I. The La-M-Cu-O (M=La,Ba,Sr and Pb) System

After the initial discovery of superconductivity over 30K in the $La_{2-x}Ba_xCuO_4$ system[1] several groups[3-6] confirmed the result both resistively and magnetically (flux expulsion). Ultimately, transitions were observed in the analagous compounds with Ba replaced with Ca[7] and Sr[7,8] for $0.1 \le x \le 0.3$ with the highest $T_c$'s above 40K.

Our samples were prepared from reagent grade powders of $La_2O_3$, $BaCO_3$, $SrCO_3$, $CaCO_3$, $PbO_2$, and CuO. The powders were mixed in appropriate ratios and calcined in air between 1000C and 1100C for 12 hours. The resulting materials were reground, pressed into small disks (nominally 1cm. diameter by 2mm. height) and sintered in air at 1000C-1100C for 12h. The calcined powders and sintered pellets were x-rayed following each process to ensure that the proper phase was present.

The La-Ba-Cu-O compounds were prepared in three compositions, $La_{2-x}Ba_xCuO_4$ where x=0.1, 0.2, and 0.3. The resistive transitions were measured on the sintered pellets by attaching four leads with indium solder. The resistivity of the pellets was ~$10^4$ $\mu\Omega$-cm. This high value was probably due to the granularity of the poorly sintered samples rather than the intrinsic resistivity of the materials themselves. This is consistent with the generally broad transitions and low (~5A/cm$^2$) critical currents of the samples. Figure 1 shows the resistive and magnetic transitions for the x=0.1 sample which had the sharpest transition and the highest onset temperature. The onset temperature $T_0$ was 40K and the signal dropped below instrument noise (which will be called R=0) at 24K. The magnetic moment, measured while cooling in a 100G ambient field, was still changing at 10K (the lowest temperature measured)

where it represented ~10% flux expulsion (subsequent Sr samples showed over 50% expulsion). The magnetic onset temperature was ~28K.

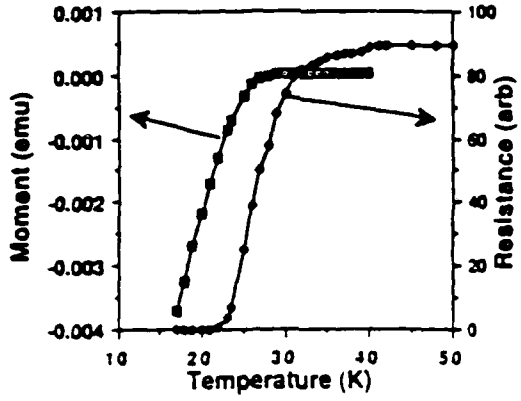


FIG. 1. Resistance and magnetic moment plotted vs temperature of $La_{1.9}Ba_{0.1}CuO_4$. The onset temperature for superconductivity in the resistive transition is 40 K. Magnetic moment was measured cooling in 100 Oe and represents about 10% flux exclusion.

Magnetic transitions for $La_{1.8}Sr_{0.2}CuO_4$ and $La_{1.7}Ca_{0.3}CuO_4$ are shown in Figure 2. Their magnetic transitions are at 36 and 24K respectively. Samples with Ba and x=0.1 and 0.2; Sr with x=0.1 and 0.2; and Ca with x=0.3, showed x-ray spectra (Figure 3) characteristic of nearly single phase $K_2NiF_4$ structure (Figure 4) and had higher and sharper transitions than other compositions.



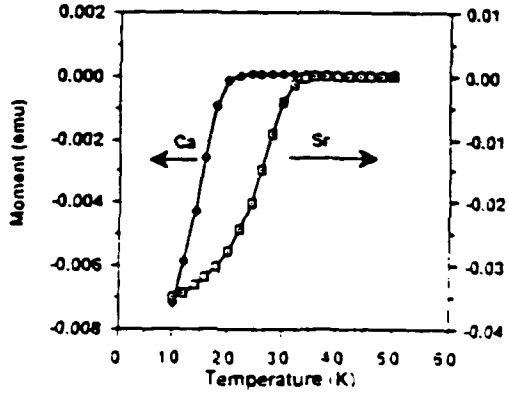


FIG. 2. The magnetic moment of $La_{1.8}Sr_{0.2}CuO_4$ and $La_{1.7}Ca_{0.3}CuO_4$ plotted vs temperature. The magnetic moment for the sample at 10 K represents almost 60% flux expulsion (100-Oe applied field).

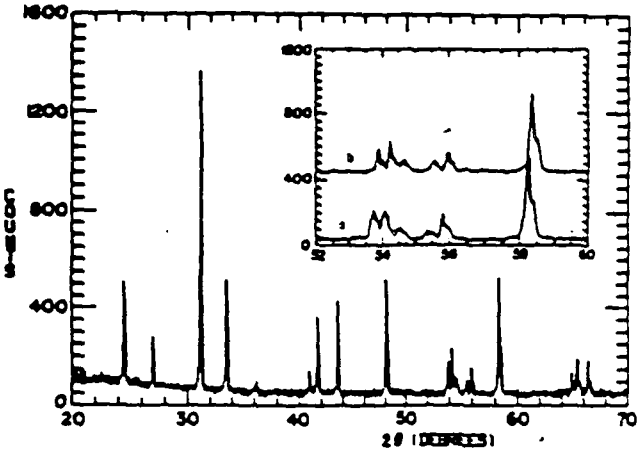


FIG. 3. The x-ray powder diffraction pattern for the twice-calcined sample of $La_{1.9}Ba_{0.1}CuO_4$. The pattern shows a single-phase $K_2NiF_4$ structure. The inset compares a portion of this pattern [(b) upper trace] with the same region of the x-ray pattern for the (a) singly calcined sample. Note that the singly calcined sample has broader lines at a slightly smaller $2\theta$ (indicating a larger lattice parameter).

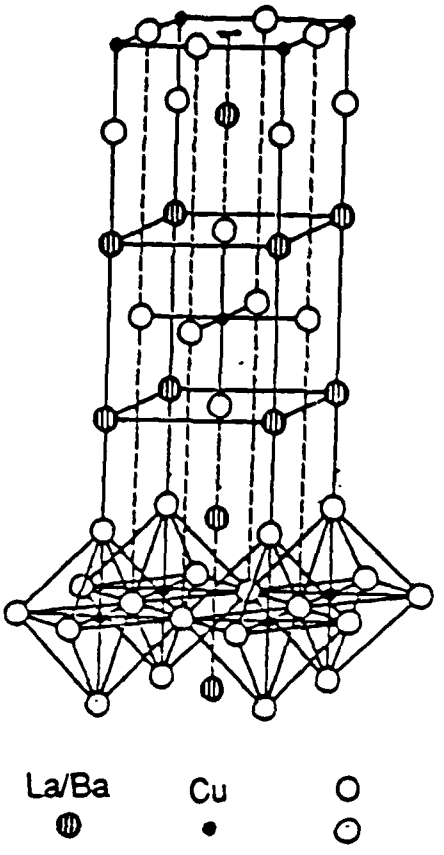


Fig. 4 The tetragonal $K_2NiF_4$ structure.
(From Longo and Raccah, 1973)

Three compositions of $La_{2-x}Pb_xCuO_4$ with x=0.1, 0.2, and 0.3 were also made. These samples were processed as the others. The x=0.1 sample's x-ray spectrum showed a nearly single phase $K_2NiF_4$ structure. However, these samples showed activated conductivity with no sign of superconductivity. Various subsequent annealing procedures were attempted to improve the behavior. An inert gas anneal at 750C for 12h produced the lowest resistivity (~30,000 Ω-cm) but , again, there was no sign of superconductivity.

Superconductivity in this new class of high $T_c$ compounds appears to be intimately connected with the valence of the $Cu^{3+}$ ion[7]. In $La_2CuO_4$ the copper is in the +2 valence state. The addition of Ba, Sr, Ca, and Pb either forces some of the Cu ions into the +3 valence state, creating a mixed valence compound, or produced oxygen vacancies[9,10]. The preservation of $Cu^{3+}$ by minimizing the oxygen vacancy formation

with suitable processing procedures is essential to superconductivity. The extra electrons from Cu provide carriers which make the materials highly conductive and sometimes superconductive. The relative amounts of $Cu^{3+}$ ions can be inferred from the x-ray structural analysis. $Cu^{3+}$ produces an expansion of the c parameter relative to the a parameter if the oxgen content remains constant[10]. Table 1 lists the a and c parameters for the compounds shown as well as the $T_0$ values of the samples. The correlation of superconductivity with the size of the c/a ratio is clear.

TABLE I. Sample parameters.

| Material | $a$ (Å) | $c$ (Å) | $c/a$ | $T_0$ (K) |
|---|---|---|---|---|
| $La_{1.8}Ca_{0.2}CuO_4$ | 3.790 | 13.159 | 3.47 | 22.5 |
| $La_{1.7}Ca_{0.3}CuO_4$ | 3.782 | 13.162 | 3.48 | 25 |
| $La_{1.9}Ba_{0.1}CuO_4$ | 3.786 | 13.238 | 3.49 | 30[a] |
| $La_{1.9}Ba_{0.1}CuO_4$ | 3.787 | 13.256 | 3.50 | 33[a] |
| $La_{1.8}Ba_{0.2}CuO_4$ | 3.801 | 13.301 | 3.50 | 31 |
| $La_{1.9}Sr_{0.1}CuO_4$ | 3.771 | 13.233 | 3.51 | 36.5 |
| $La_{1.8}Sr_{0.2}CuO_4$ | 3.777 | 13.261 | 3.51 | 37 |
| $La_{1.7}Sr_{0.3}CuO_4$ | 3.798 | 13.111 | 3.45 | < 4 |
| $La_{1.9}Pb_{0.1}CuO_4$ | 3.801 | 13.191 | 3.47 | . . . |
| $La_{1.8}Pb_{0.2}CuO_4$ | 3.772 | 13.120 | 3.48 | . . . |
| $La_{1.7}Pb_{0.3}CuO_4$ | 3.791 | 13.158 | 3.47 | . . . |

[a] $T_0$ measured by dc susceptibility.

Reacting or annealling the compounds in oxygen can be either detrimental or beneficial depending on the presence of second phase higher order oxides. If higher order oxides are present then annealing in oxygen at high temperatures will promote the growth of these phases at the expense of the desired phase. An associated reduction of the c parameter is then observed. In this situation , annealling in a reducing atmosphere rather than an oxidizing one promotes the growth of $La_{2-x}M_xCuO_4$ oxide and enhances the superconducting properties. If, on the other hand, one has a single phase $K_2NiF_4$ structure or a second phase of lower oxides, then a low temperature oxygen anneal which does not nucleate a higher oxide second phase will promote the formation of more $Cu^{3+}$ by ensuring that more oxygen vacancies are filled.

## II. The Y-Ba-Cu-O system

Soon after the discovery of superconductivity above 90°K in the Y-Ba-Cu-O system[2] several groups[11-17] identified the superconducting phase and its crystal symmetry using electron and x-ray diffraction. Although all investigations agreed on the $YBa_2Cu_3O_{9-\delta}$ stoiciometry for the compound and the position of the metal cations in the unit cell, there was disagreement as to whether the symmetry is tetragonal[11,12,17] or orthorhombic[13-16] and to the location and occupation of the oxygen sites. This section reports on neutron diffraction studies performed on our samples in a collaboration with a group at The National Bureau of Standards[18]. These measurements determined the oxygen positions and occupation in the unit cell. We then report on a study which relates the positions and occupation of these oxygens to processing procedures and correlate that result to superconducting behavior.

The materials for the neutron study were prepared from 99.9% purity $Y_2O_3$, CuO, and $BaCO_3$ powders which were mixed to a nominal composition of $YBa_2Cu_3O_x$. The powders were predried to remove adsorbed water and then carefully premixed to break up agglomerates. The premixed powders were calcined at 900-950°C for about 6 hours with hourly intermediate grindings. The degree of chemical reaction was monitored with x-rays. The calcined powders were then ground and cold pressed into 1-2 gram pellets and sintered for 12 hours at 937°C. The samples were finally annealed in oxygen at 900°C for three hours and then furnace cooled at 1° per minute to 300°C. Individual pellets were characterized with x-ray diffraction and found to be identical. The samples were examined for superconductivity by four probe resistance measurements and by dc magnetic susceptibility. The resistance data (Figure 5) showed the first deviation from linear temperature dependence above 115°K. Between 115° and 93° the resistance drops about 10% from a straight line extrapolation of the high temperature data. At 93°K the resistance sharply drops and is in the instument noise by 91°. The (field cooled) magnetic moment measured in a dc field of 100 gauss is shown in Figure 6 and shows a diamagnetic onset at 92°K. The transition is complete around 30° and corresponds to over 60% flux expulsion. Geometric considerations limit the precise determination of this fraction.

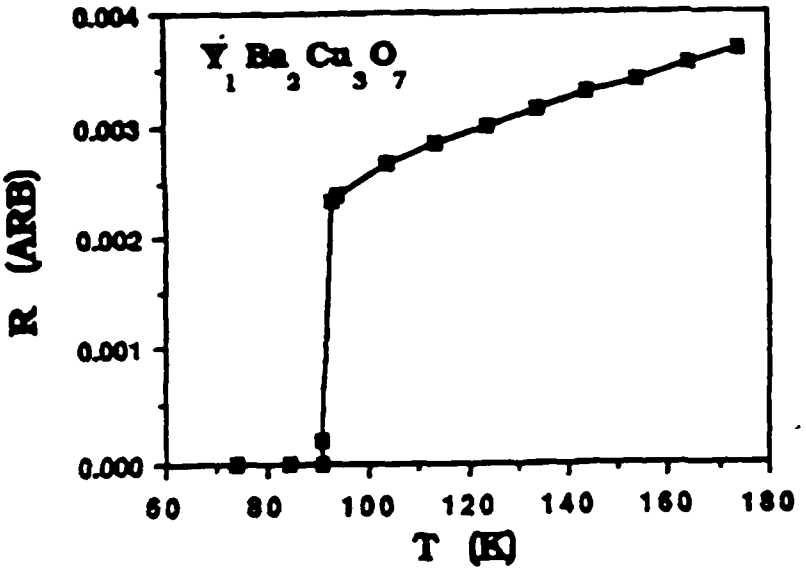


Fig. 5 Temperature dependence of the resistance of $Y_1Ba_2Cu_3O_7$.

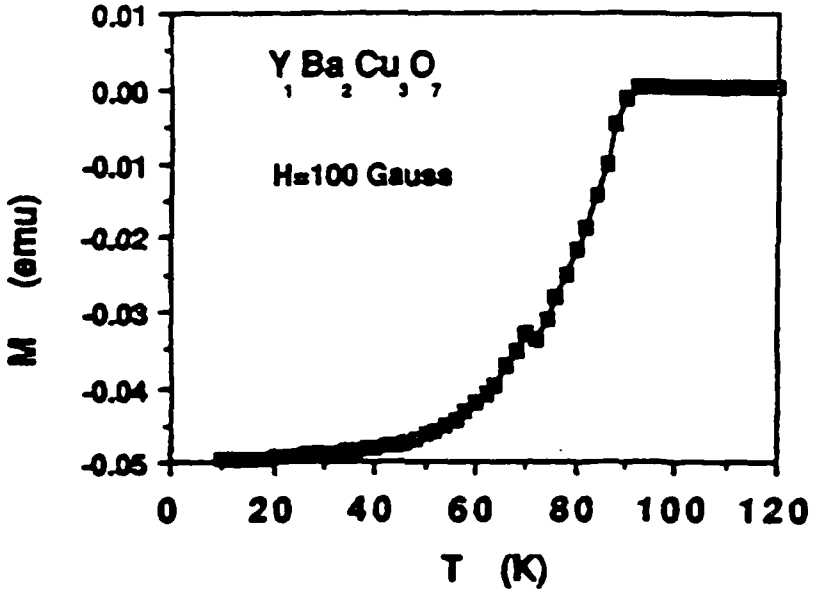


Fig. 6 Temperature variation of the magnetization. The sample was cooled in a 100 gauss field.

Unlike x-ray diffraction, neutron diffraction is strongly sensitive to the oxygen atoms which allows a precise determination of both oxygen position and occupation in the unit cell of these compounds. The refinement[18] of the powder diffraction data taken at the National Bureau of Standards reactor determined that the compound has orthorhombic symmetry of space group Pmmm, and that the stoiciometry of the compound was $YBa_2Cu_3O_{6.95}$ with an uncertainty of 0.01 in the oxygen composition.

The lattice parameters ($a_0$=3.8220Å, $b_0$=3.8855Å, and $c_0$=11.6797Å) and atomic positions determined from the refinement were essentially identical to those found by Beech et al.[19] from a similar sample. The structure is shown in Figure 7. The essential features are that the copper atom Cu(1) is located at the center of a distorted rectangle formed by two O(4) atoms and two O(1) atoms. This forms oxygen chains along the b axis, alternated with Cu(1) atoms. This b-axis atom configuration is responsible for the orthorhombic distortion versus the a-axis direction which does not have the oxygen chains. The second Cu site, Cu(2), is also surrounded by four oxygen atoms in sites O(2) and O(3) which are almost coplanar and form a tetrahedron with the O(1) site. The Cu(2) atom is slightly displaced from the oxygen plane. The O(1), O(2), and O(3) sites are fully occupied while the O(4) site contains a small deficiency of 0.05 atom (total oxygen concentration is 6.96 atoms/formula unit). These results are consistent with other results[19,20].

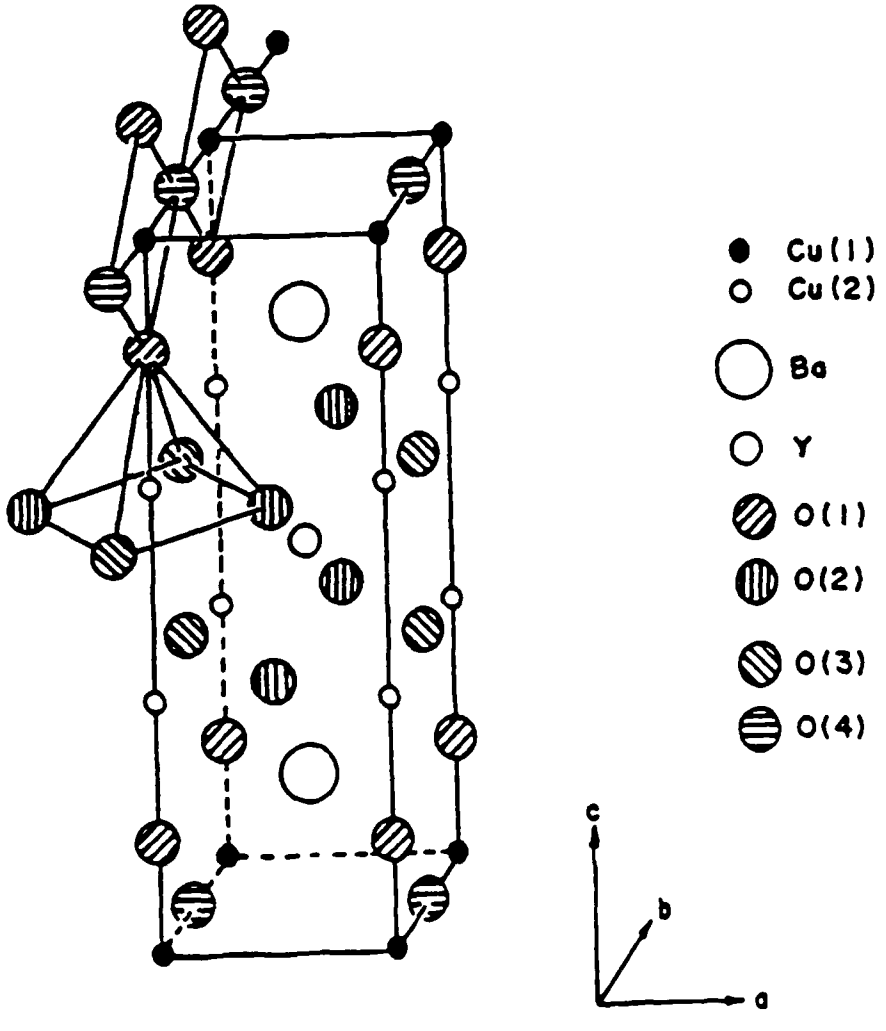


Fig. 7 Structure of the compound as determined from neutron diffraction (From reference 19)

During the course of our early work[11] we studied about 20 samples of different compositions all containing the 1:2:3 (Y:Ba:Cu) phase. As there were no well defined optimum processing procedures at that time, we prepared samples by several different techniques. We observed the orthorhombic structure in about half of the samples and the tetragonal in the other half. Reviewing these results in light of the refined crystal structure, clarifies the relationships between processing and structure.

Processing conditions which favored the formation of the orthorhombic structure were described above. The last step (slow cool in oxygen) could be replaced with an equilibration at 950°C in oxygen or air, followed by reducing the temperature to 500-700°C, holding for several hours and a moderately slow cool down.

Two conditions favored the tetragonal formation. When the processing was done at relatively low temperatures and shorter times, the chemical reactions and subsequent grain growth were incomplete, the ordering of the oxygen atoms did not occur and a tetragonal phase was observed. In cases where the reaction was known to be complete (from x-rays), the tetragonal phase was formed when samples were quenched from 900-1000°C.

Most of these early samples were prepared off the stoiciometric 1:2:3 and we observed the orthorhombic and tetragonal symmetries with nearly equal frequency. We saw no obvious correlation between overall composition and the occurrence of either phase. At the stoiciometric composition we observed only the orthorhombic structure. There was no indication, however, that the tetragonal phase has a stoiciometry other than 1:2:3.

Table 2 shows the lattice parameters of some of the samples. These parameters were calculated assuming the structure to be orthorhombic and carrying out a least squares fit to 15 to 20 high angle diffraction peaks. If the "a" and "b" parameters were determined to be equivalent to within the uncertainty of the fit , we called the sample tetragonal. For all the samples determined to be orthorhombic, the b/a ratios lie between 1.014 and 1.019. The "a" lattice parameter varies varies from 3.822 to 3.838. The "b" parameter varies from 3.879 to 3.911. For nearly tetragonal samples, the orthorhombic distortion ranges from less than measurable to about 0.25% with the "a" parameter varying from 3.863 to 3.876 and the "b" from 3.867 to 3.877.

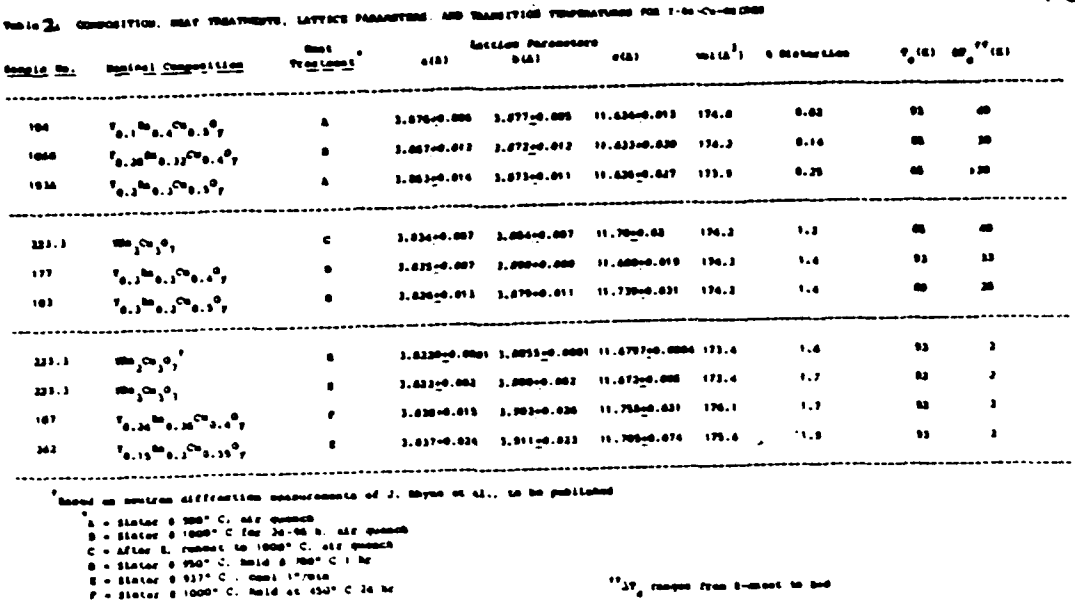

For the samples we tested there was no overlap of the b/a ratios between the two groups of samples; ie. the distortion was 1.4-1.9% in the orthorhombic samples and less than 0.3% in the tetragonal samples. The "b" parameter tends to be slightly smaller in the tetragonal structure compared to the orthorhombic, whereas "a" clearly shows the opposite trend. This would indicate at least partial occupancy of both 1/2,0,0 and 0,1/2,0 sites in the tetragonal structure. Thus we regard the tetragonal structure as the disordered form of the orthorhombic lattice.

We made four point resistiance dc susceptibility measurements on the samples. The resistive onsets occurred in excess of 90°K in most samples. Slow cooling and/or annealing at about 500°C, in either oxygen or air, sharpens the transitions, in agreement with others[21,22]. Stoiciometric 1:2:3 compositions and well defined orthorhombic distortions had 93-91°K resistive transitions with major fractions of the samples expelling flux. Samples containing the tetragonal phase show much broader transitions and smaller volume fractions expelling flux. The sample with the least distortion, sample 194, had the broadest transition 93-53°K (Figure 8). Samples with a distortion of about 1.4% but which were not slow cooled or held at a lower intermediary temperature, had high onsets but broad transitions. Thus only those samples that were slow cooled or held at a lower temperature had sharp transitions suggesting that slow cooling allows more complete ordering of oxygen atoms on the 0,1/2,0 sites. The results of the off-stoiciometric samples are somewhat complicated by their mixed phase nature. The resulting materials consist of superconducting Islands imbedded in an insulating matrix. Such systems have broad transitions due to

Josephson tunnelling between superconducting regions and may have $T_c$'s which are lower than the superconductor.

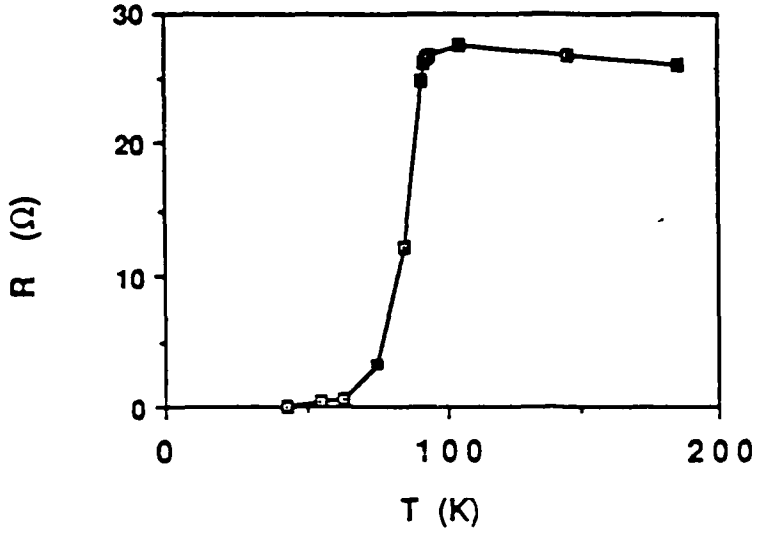


Fig. 8 Resistance vs. temperature for sample 194 ($Y_{0.6}Ba_{2.4}Cu_3O_y$).

To clarify the relationship between orthorhombic and tetragonal symmetry, we used a stoiciometric sample, 223.3, with a $1.017_3$ distortion. After equilibration at 1000°C we quenched the sample in air. There was no change in "b" or "c" but about a 0.3% increase in "a" which gives a 1.013 distortion. It is difficult to unambiguously resolve the tetragonal from the orthorhombic phases. We are probably left with a system that can be modelled as a superconducting orthorhombic phase imbedded in an insulating tetragonal phase. The resistance increases (since the tetragonal phase is an insulator) and, as before, the onset temperature decreases and the transition broadens. Figure 9 shows that the transition went from 93-91°K before quench to 85-46°K after.

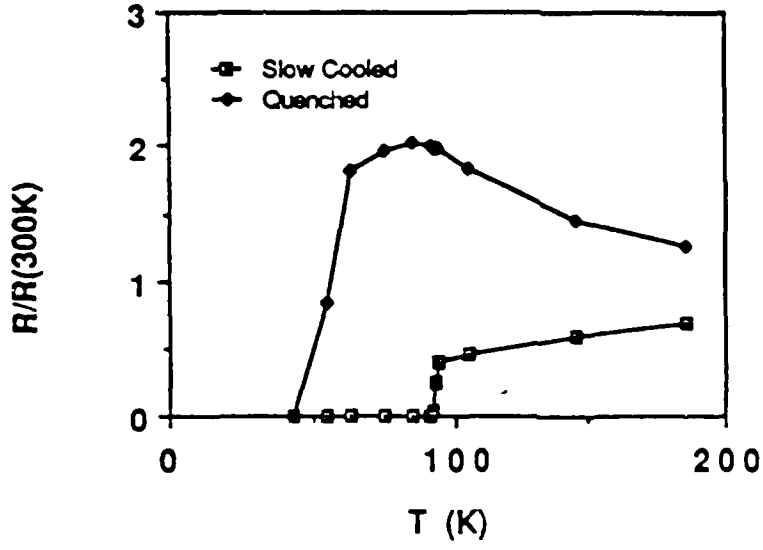


Fig. 9 Resistance vs. temperature for sample 223.3 ($YBa_2Cu_3O_7$) comparing the transition after being slow cooled and quenched.

The conversion from the orthorhombic to the tetragonal phases can occur by disordering and/or removing oxygen atoms from the 0,1/2,0 positions. This has been shown[23,24] by heating a sample in a reducing atmosphere and observing the oxygens with neutron diffraction. Oxygen atoms were removed preferentially from the 0,1/2,0 sites until the sample eventually became semiconducting.

The (now well verified) result is that the orthorhombic distortion occurs on slow cooling or holding at some lower intermediary temperature[21-25] when oxygen atoms diffuse from 1/2,0,0 sites to vacant 0,1/2,0 sites and by the addition of oxygen atoms from the ambient atmosphere. It is well known that related compounds will incorporate 10-15% more oxygen during a low temperature post anneal[26]. It is also clear that superconductivity is strongly dependent on the presence of the Cu-O chains in the basal plane of the structure.

## III. Transitions above 200°K(?)

Since the discovery of the 90°K superconductors researchers have reported higher temperature resistance drops which they believed to be minority super high temperature superconducting phases. Generally the processing procedures used to obtain such samples involve 'abusing' the samples or making them off the 1:2:3 stoiciometry and the "transitions" disappear after thermal cycling. Recently, Huang et al.[27] reported the observation of a sharp drop in resistance at 230°K in an argon treated specimen of $EuBa_2Cu_3O_{6+\delta}$. In this section we report on a resistance drop at temperatures above 200°K which occur in $YBa_2Cu_3O_{6+\delta}$ samples similarly treated in argon which is not due to superconductivity.

The $YBa_2Cu_3O_{6+\delta}$ samples were made as described above and were orthorhombic as determined by x-ray diffraction. Most of the samples had good sharp transitions (93-91°K) before argon treatment. The samples were pumped for several hours in a vacuum of better than $10^{-6}$ torr at room temperature and then exposed to flowing argon, again at room temperature, for several hours. The details for various specimens are given in table 3. All of these specimens showed qualitatively similar resistivity behavior with temperature.

| Experiment # | Specimen # | Composition | Time for Pumping | Time for Argon Exposure | Remarks |
|---|---|---|---|---|---|
| 1 | L-1 | $Y_\delta$-Ba$_2$Cu$_3$O$_x$ | 24 hr | 24 hr | |
| 2 | L-1 | $Y_\delta$-Ba$_2$Cu$_3$O$_x$ | 24 hr | 72 hr | |
| 3 | L-1 | $Y_\delta$-Ba$_2$Cu$_3$O$_x$ | - | - | Resistance measured again after removing surface layer by sandpaper. |
| 4 | L-1 | $Y_\delta$-Ba$_2$Cu$_3$O$_x$ | - | - | Resistance measured after second rubbing with sand paper. |
| 5 | A-1 | $Y_\delta$-Ba$_2$Cu$_3$O$_x$ | 24 hr | 72 hr | |
| 6 | C-1 | $Yb_{1-y}Nd_{0.1}$Ba$_2$Cu$_3$O$_x$ | 24 hr | 72 hr | |
| 7 | C-2 | $Yb_{1-y}Nd_{0.1}$Ba$_2$Cu$_3$O$_x$ | 24 hr | 72 hr | |

Table 3. Details of Argon treatment for various specimens.

Indium contacts were soldered to the samples for four-probe, ac (26.5hz) resistance measurements. Figure 10 shows R(T) for specimen L-1. The measurements, made with 50, 500 and 5000μA currents, show a sharp superconducting transition (between 91 and 93°K) to a resistance of 2mΩ. The resistance increases linearly to a value of 4mΩ at around 250°K where the curves for the three currents separate. The 50μA data shows a substantial resistance increase which peaks a about 275°K. The higher current data shows much smaller resistance increases. The measurements were made both warming and cooling the sample. A final 50μA room temperature resistance measurement , made before removing the sample from the cryostat, agreed with the initial 50μA resistance. The measurements were repeated on the sample after the top millimeter was sanded off as well as on several other samples. These curves had the same general behavior with the peak in the 50μA resistance varying from 275°K to over 300°K.

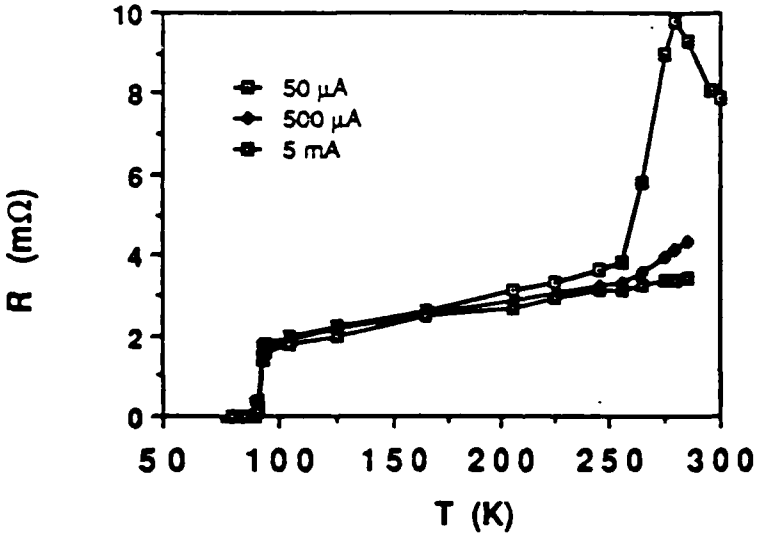


Fig. 10 Resistance Vs. temperature for argon treated $YBa_2Cu_3O_7$ measured with 50 500 and 5000μA currents.

As stated before, others have attributed such large resistance changes above 200°K to extra-high $T_c$ superconducting filaments. This is unlikely here since our data shows the high temperature resistance decreasing with large currents rather than the low temperature resistance increasing as would be expected from exceeding the critical current of the filaments. This conclusion is consistent with magnetization versus

temperature measurements (Figure 11). The sample shows a virtually flat magnetic signal from 300°K to 93°K where the diamagnetic onset occurs. From the magnetude of the signal at 50° we estimate approximately 5% flux expulsion. Magnifying the curve between 200 and 300°K (inset) shows a very weak increase in the signal with decreasing temperature and no hint of diamagnetism. The points between 93° and 300° have 10% uncertainties.

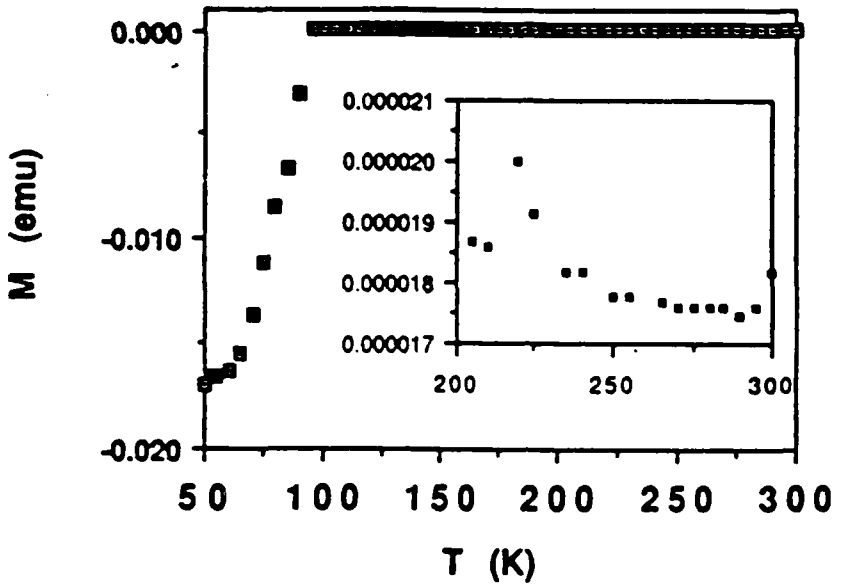


Fig. 11 Magnetization vs. temperature for argon treated $YBa_2Cu_3O_7$ showing a diamagnetic onset at 93K and no diamagnetic shift above 200K (inset). The points above 93K have a 5-10% uncertainty.

The anomalous resistance drop may be explained in terms of a semiconductor-metal transition. Testardi et al.[28] have detected a discontinuity in static dielectric constant at 220°K (seen both on cooling and heating). Jezowski et al.[29] have measured electrical resistivity as well as thermal conductivity of single phase $YBa_2Cu_3O_y$ between 5° and 320°K. The electrical resistivity was linear in the normal state up to the highest measured temperature but they did detect a small departure from a linear dependence between 200 and 260°K. It should also be noted that a change of slope in the temperature dependence of the thermopower has been seen in this temperature range[29].

Based on these observations , we propose that the resistance anamoly is most likely associated with an order-disorder transition of oxygen on or near the grain boundaries of the orthorhombic grains (with $T_c$~93°K). When the specimens are subjected to long term vacuum or argon anneals, even at room temperature, oxygen on or near grain boundaries is partially depleted, forming a tetragonal-like 'phase' which adds excess resistance between the grains. The result is a sample with a larger total resistance (since the tetragonal 'phase' is an insulator) and an activated temperature dependence near 300°K due to hopping conduction between the grains.

A recent study[30] determined the dependence of the tetragonal to orthorhombic transition on temperature and oxygen content. Extrapolating their data shows this transition could occur at room temperature for $YBa_2Cu_3O_{6.8}$.

Therefore, at some temperature (below room temperature) oxygen and vacancies order, the tetragonal 'phase' reverts to an orthorhombic structure, the grain boundary regions become metallic, the resistance decreases to a value close to the intrinsic resistivity of the material and the specimen shows a resistive anomaly. This is not superconductivity but a change of the grain boundaries from insulating to conducting behavior.

## Acknowledgements

I would like to acknowledge the sponsorship of the Office of Naval Research (ONR), the Office of Naval Technology (ONT) and the Defense Advanced Research Project Agency (DARPA). I would also like to thank the many collaborators who have contributed to NRL's High Temperature Superconductivity Program.

## References

1 J. G. Bednorz and K. A. Muller, Z. Phys. B64, 189 (1986)

2 M. K. Wu, J. R. Ashburn, C. J. Torng, P. H. Hor, R. L. Meng, L. Gao, Z. J. Huang, Y. Q. Wang, and C. W. Chu, Phys. Rev. Lett. **58**, 908(1987)

3 C. W. Chu, P. H. Hor, R. L. Meng, L. Gao, Z. J. Huang, and Y. Q. Wang, Phys. Rev. Lett. **58**, 405 (1987)

4 S. Uchida, H. Takagi, K. Kitazawa, and S. Tanaka, Jpn. J. Appl. Phys **26**, L1 (1987)

5 H. Takagi, S. Uchida, K. Kitazawa, and S. Tanaka, Jpn. J. Appl. Phys **26**, L123 (1987)

6 S. Uchida, H. Takagi, K. Kitazawa, and S. Tanaka, Research Report on New Superconducting Materials (Special Project Research No. 106 Ministry of Education, Science and Culture) March 15, 1987

7 R. J. Cava, R. B. van Dover, B. Batlogg, and E. A. Rietman, Phys. Rev. Lett. **58**, 408 (1987)

8 K. Kishio, K. Kitazawa, S. Kanbe, I. Yasuda, N. Sugii, H. Takagi, S. Uchida, K. Fueki, and S. Tanaka, Chem. Lett., 429 (1987)

9 N. Nguyen, J. Choisnet, M. Hervieu, and B. Raveau, J. Solid State Chem. **39**, 120 (1981)

10 C. Michel and B. Raveau, Rev. Chim. Miner. **21**, 407 (1984)

11 S. B. Qadri, L. E. Toth, M. Osofsky, S. Lawrence, D. U. Gubser, and S. A. Wolf, Phys. Rev. **B35**, 7235(1987)

12 R. M. Hazen, L.W. Finger,R. J. Angel, C. T. Prewitt, N. L. Ross, H. K. Mao, C. G. Hadidiacos, P. H. Hor, R. L. Meng, and C. W. Chu., Phys. Rev. **B35**, 7238(1987)

13 R. Beyers, G. Lim, E. M. Engler, R. J. Savoy, T. M. Shaw, T. R. Dinger, W. J. Gallagher, and R. L. Sandstrom, Appl. Phys. Lett. **51**, 614(1987)

14 Y. Lepage, W. R. McKinnon, J. M. Tarascon, L. H. Greene, G. W. Hull, and D. M. Hwang, Phys. Rev. **B35**, 7245(1987)

15 Y. Syono, M. Kikuchi, K. Oh-ishi, K. Hiraga, H. Arai, Y. Matsui, N. Kobayashi, T. Sasaoka, and Y. Muto, Jpn. J. Appl. Phys **26**, L498 (1987)

16 R. J. Cava, B. Batlogg, R. B. van Dover, D. W. Murphy, S. Sunshine, T. Seigrist, J. P. Remeika, E. A. Reitman, S. Zahurak, and G. P. Espinosa, Phys. Rev. Lett. **58**, 1676(1987)

17 M. Hirabayashi, H. Ihara, N. Terada, K. Senzaki, K. Senzaki, K. Hayashi, K. Murata, M. Tokumoto, S. Waki, and Y. Kimura, Jpn. J. Appl. Phys **26**, L454 (1987)

18 J. J. Rhyne, D. A. Newmann, T. A. Gottaas, F. Beech, L. Toth, S. Lawrence, S. Wolf, M. Osofsky, and D. U. Gubser, Phys. Rev. **B36**, 2294(1987)

19 F. Beech, S. Miraglia, A. Santoro, and R. S. Roth, Phys. Rev. **B35**, 8778(1987)

20 M. A. Beno, L. Soderholm, D. W. Capone II, D. G. Hinks, J. D. Jorgensen, I. K. Schuller, C. U. Segre, K. Zhang, and J. D. Grace, Appl. Phys. Lett. **51**, 57(1987)

21 J. D. Jorgensen, B. W. Veal, W. K. Kwok, G. W. Craptree, A. Umezawa, L. J. Nowicki, and A. P. Paulikas, Phys. Rev. **B36**, 5731(1987)

22 J. M. Tarascon, W. R. McKinnon, L. H. Greene, G. W. Hull, and E. M. Vogel, Phys. Rev. **B36**, 226(1987)

23 J. D. Jorgensen, M. A. Beno, D. G. Hinks, L. Soderholm, K. J. Volin, R. L. Hitterman, J. D. Grace, I. K. Schuller, C. U. Segre, K. Zhang, and M. S. Kleefisch, Phys. Rev. **B36**, 3608(1987)

24 L. H. Greene, Private communication

25 E. M. Engler, V. Y. Lee, A. I. Nazzal, R. B. Beyers, G. Lim, P. M. Grant, S. S. P. Parkin, M. L. Ramirez, J. E. Vazquez, and R. J. Savoy, J. Amer. Chem. Soc.

26 L. Eh-Rakho, C. Michel, J. Provost, and B., Raveau, J. Solid State Chem. **37**, 151 (1981)

27 C. Y. Huang, L. J. Dries, P. H. Hor, R. L. Meng, C. W. Chu, and R. B. Frankel, Nature **328**, 403(1987)

28 L. R. Testardi, W. G. Moulton, H. Mathias, H. K. Ng, and C. M. Rey, (Submitted to Phys. Rev. Lett.)

29 A. Jezowski, J. Mucha, K. Rogacki, R. Horyn, Z. Bukowski, M. Horobiowski, J. Rafalowicz, J. Stepien-Damm, C. Sulkowski, E. Trojnar, A. J. Zaleski, and J. Klamut, Phys. Lett., 431 122 (1978)

30 A. T. Fiory, M. Gurvitch, R. J. Cava, and G. P. Espinosa, (submitted to Phys. Rev. B)

END
DATE
FILMED
4-88
DTIC